

CHEMICAL AND ISOTOPIC CHARACTERISTICS OF THE COSO EAST FLANK HYDROTHERMAL FLUIDS: IMPLICATIONS FOR THE LOCATION AND NATURE OF THE HEAT SOURCE

Bruce W. Christenson¹, B. Mack Kennedy², Michael C. Adams³, Steven C. Bjornstad⁴ and Cliff Buck⁵

¹GNS Science, National Isotope Centre
PO Box 31-312, Lower Hutt, NEW ZEALAND
e-mail:b.christenson@gns.cri.nz

²Lawrence Berkeley National Laboratory, Centre for Isotope Geochemistry
1 Cyclotron Road, Berkeley CA, 94720

³2889 Millicent Dr., Salt Lake City Utah 84108.

⁴Geothermal Program Office, Naval Air Weapons Station
China Lake, CA 93555

⁵Coso Operating Company, Coso Junction, CA 93555

ABSTRACT

Fluids have been sampled from 9 wells and 2 fumaroles from the East Flank of the Coso hydrothermal system with a view to identifying, if possible, the location and characteristics of the heat source inflows into this portion of the geothermal field. Preliminary results show that there has been extensive vapor loss in the system, most probably in response to production. Wells 38A-9, 51-16 and 83A-16 show the highest CO₂-CO-CH₄-H₂ chemical equilibration temperatures, ranging between 300-340 °C, and apart from 38A-9, the values are generally in accordance with the measured temperatures in the wells. Calculated temperatures for the fractionation of ¹³C between CO₂ and CH₄ are in excess of 400 °C in fluids from wells 38A-9, 64-16-RD2 and 51A-16, obviously pointing to equilibrium conditions from deeper portions of the reservoir. Given that the predominant reservoir rock lithologies in the Coso system are relatively silicic (granitic to dioritic), the isotopic signatures appear to reflect convective circulation and equilibration within rocks close to the plastic-brittle transition. ³He/⁴He signatures, in conjunction with relative volatile abundances in the Coso fluids, point to a possibly altered mantle source for the heat source fluids.

INTRODUCTION

On a regional scale, hydrothermal system fluids associated with magmatic heat sources carry

geochemical and isotopic signatures which provide insights into the deeper crustal processes operating in the magmato-tectonic provinces from which they derive (eg. Fischer and Marty, 2005; Hilton, 1996; Giggenbach, 1995). The heat source at Coso is of particular interest in this regard owing to the relatively shallow nature of the plastic-brittle transition (4 – 5 km, Lees, 2002), and the fact that it is situated in a tectonically complex environment which has resulted in crustal thinning, and appears to show strong asthenospheric influence on the hydrothermal system fluid compositions (Monastero et al., 2005).

On a smaller scale, isotopic and geochemical signatures also provide valuable information about physical reservoir processes in geothermal reservoirs, and location(s) of source inflows into geothermal fields (Christenson et al., 2002, Kennedy & Truesdell, 1996). Such information is of course invaluable for resource exploration and development programs.

A key motivation for this work has been to provide information that could assist with future EGS developments within the East Flank compartment of the Coso system, where it is reasoned that knowledge of natural heat source inflows and recharge pathways could augment such development.

SAMPLING AND ANALYSIS

A total of 9 production wells (Fig. 1) and two fumarolic discharges (West Canyon Fumarole, WCF and Steamline Fumarole, SLF) were sampled on the East Flank in May 2005. In addition, one high-temperature well each from the Navy I (68-6) and the BLM West (23-19-RD) compartments were sampled for comparative purposes. Waters were chemically analyzed at GNS Science (NZ) for routine major constituents, including ^{18}O and ^2H . Major and trace volatiles were also chemically analyzed at GNS Science, stable isotopes of C, N and O were analyzed at Isotrace NZ Ltd., and noble gas isotopes were analyzed at the LBNL Centre for Isotope Geochemistry.

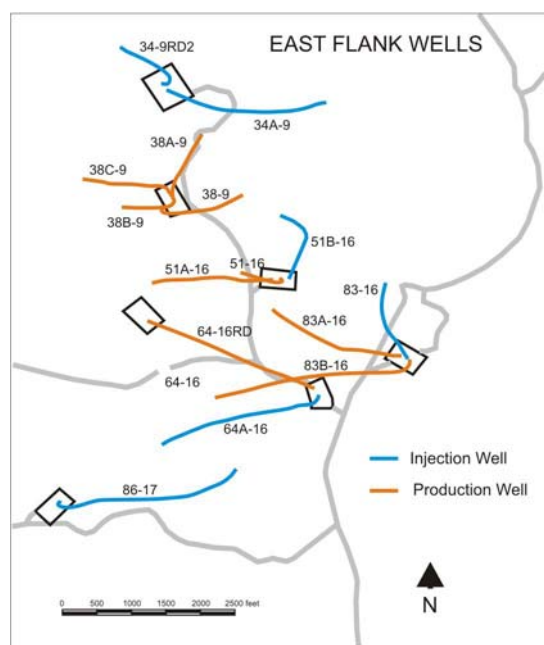


Figure 1. Location map for wells on the East Flank of the Coso system.

SUMMARY OF RESULTS

Water Chemistry

Evidence suggests that exploitation of the field has affected the compositions of *liquid-phase* samples in this study to such an extent that very little information pertinent to the identification of source fluid inflows into the East Flank can be derived from them. Owing to insufficient recharge, field operational strategy entails injection of flashed production brines back into the reservoir via injector wells (Fig. 1), and significant but presently unquantified injection returns have been recognized in all wells apart from 38C-9 and 38D-9.

Fortunately, and in contrast to earlier practice in other parts of the system, off-gases have not been injected

into the East Flank reservoir. Therefore, dilution by injectate waters, and in some cases extensive boiling, are the only processes affecting volatile compositions on the East Flank. Whereas dilution will affect some gas-water equilibria, for the purposes of this exercise, the effect is assumed to be minor.

Well	T_{qz} ($^{\circ}\text{C}$)	H_m (kJ/kg)	Y_{res}	Cl^* (mg/l)
23-19-RD	299	2341	0.71	5967
38-9	284	2100	0.56	6850
38A-9	233	2100	0.61	4640
38C-9	284	1300	0.03	3138
38D-9	275	1260	0.04	3761
51-16	278	1850	0.40	8221
64-16-RD	280	1449	0.14	7252
68-6	286	1300	0.02	1690
83A-19	285	1550	0.19	6086
83B-19	277	1758	0.35	5263

Table 1. Calculated reservoir parameters for East Flank discharges. T_{qz} is the quartz solubility temperature, H_m the measured wellhead enthalpy, Y_{res} the calculated reservoir vapor mass fraction, and Cl^* is the liquid phase Cl concentration at T_{qz} .

Current downhole reservoir fluid (i.e. 2-phase) calculations were made using WATCHWORKS (Arnorsson & Sigurdsson, 1982; Klein, 2000). Key results of those calculations are listed in Table 1.

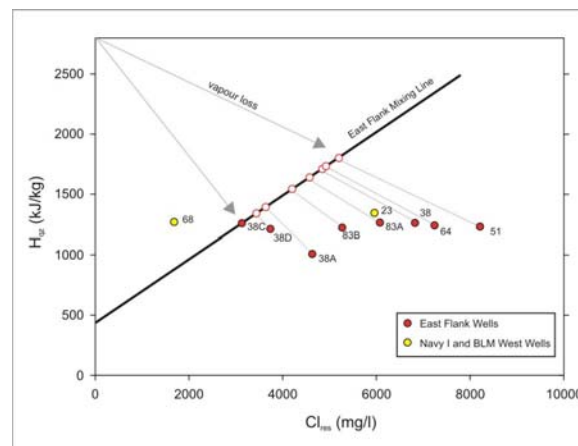


Figure 2. Chloride-enthalpy plot; Cl contents calculated at the quartz equilibrium temperature.

These results have been used to create the enthalpy – chloride diagram in Fig. 2. A system mixing line has been established for the East Flank fluids using the boiling point for pure water and the “least-boiled” composition calculated for the well 38C-9 discharge

as constraints. The highest Cl-bearing discharges lie to the south in the East Flank. Apparent vapor loss is large in some of the wells (eg. approaching 40% for 51-16), but this is a likely artifact of injectate returns to these wells. Quartz equilibrium temperatures are remarkably constant across the East Flank, with the exception of well 38A-9 which shows temperatures close to those of the maximum enthalpy for steam. It is not clear at the present time if this is an exploitation effect or natural.

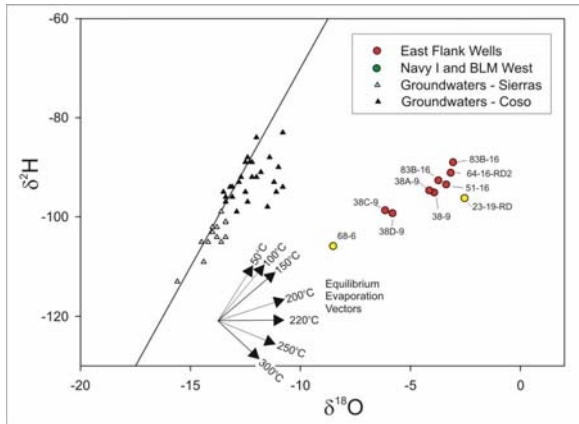


Figure 3. Water isotope data. Note positive slope for discharge trend. Vectors represent vapor-loss pathways for liquids boiling at specified temperatures.

Water isotope signatures are portrayed in Fig. 3, and even with these new data, there remains no clear resolution to the debate over the origins of the water in the Coso system. Water sourced from the Sierras (open triangles) was originally thought to predominate (Fournier and Thompson, 1982), but on the basis of further data from Coso production wells, Williams and McKibben (1990) suggested the predominance of an isotopically heavier source from the nearby Coso Range. The isotopically light signatures recoded from wells 68-6, 38C-9 and 38D-9 (Fig. 3) seemingly support recharge from the Sierras, although the data remain too few to be definitive.

Also obscuring the argument is the relatively steep, positive slope displayed by the isotopic data. This is most unusual for a single hydrothermal reservoir, given that there is very little ^2H exchange capacity in reservoir rock. The most plausible explanation for this trend is that it is the result of presently unquantified injectate returns to the East Flank wells. In this regard, ^2H can be considered a semi-quantitative indicator of injectate returns, with discharges from 38C-9 and 38D-9 least affected, 83B-16 and 64-16-RD2 most affected.

B is an excellent tracer of high temperature magmatic vapor input into hydrothermal systems (Quisfit et

al., 1989; Christenson et al., 2002), and as such, ratios of B to other conservative species such as Cl, can be useful indicators of source fluid entries into reservoirs. Initial discharge compositions for East Flank wells from the early 1990's (i.e., prior to brine injection) indicate that discharges from wells 51-16 and 83A-16 were most enriched in B, with Cl/B ratios of 31 and 14 respectively. For comparison, initial discharges from wells on pad 34 to the north had ratios >50 . Interestingly, by 2005 Cl/B ratios from 83A-16 had increased to >40 , while those from 51-16 had remained virtually constant, and the ratio for 38A-9 (previously not assessed for initial contents) is ~ 28 .

Two factors that affect our ability to interpret the Cl/B ratio as a tracer of source inputs are the hitherto unquantified effects of injectate returns to the production wells, and B transport in the vapor phase (cf. Adams, 2004). Further work is required to ascertain the effects of both processes on the current discharge compositions in order to monitor any potential changes in source fluid inflows with time. From the standpoint of the initial state of the field, it appears that principle source inflows were located in the south-central portion of the East Flank (in the vicinity of pads 51 and 83).

Gas Chemistry

There is a direct correspondence between total discharge CO_2 and calculated vapor fraction in the reservoir (Fig. 4), pointing to the influence of production-induced boiling in the reservoir. The dry steam discharge from 51A-16 has close to 12,000 $\mu\text{mol/mol}$ CO_2 , the feed for which is thought to derive from a shallow casing break in the well. At the lowest reservoir vapor fractions, total discharge

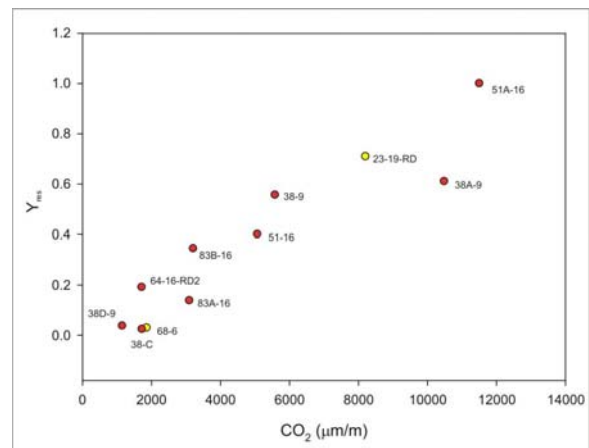


Figure 4. Total discharge CO_2 vs. reservoir vapor fraction calculated at the quartz temperature.

CO₂ contents range from 1200 to 1800 μmol/mol, and this range of values approximates fluid compositions least affected by boiling.

Relative variations in total discharge He, CO₂ and H₂S contents (Fig. 5) also provide insights into the extent to which fluids have boiled in the reservoir. The discharge from 38D-9 has the lowest CO₂/He ratio (~ 40) of any discharges, indicating that this fluid has undergone the least amount of vapor loss of any on the East Flank. Three boiling model pathways have been calculated assuming a 38D-9 “parent” fluid at 300 °C, including single-stage separation, multi-stage separation at 1° decrements, and Rayleigh separation at 300 °C. All pathways cover the range of 0 to 5% vapor loss. The distribution of data suggest that open-system degassing is the predominant boiling regime in the East Flank reservoir, with fluid from wells 38-9, 38A-9 and 51A-16 being most affected by this process.

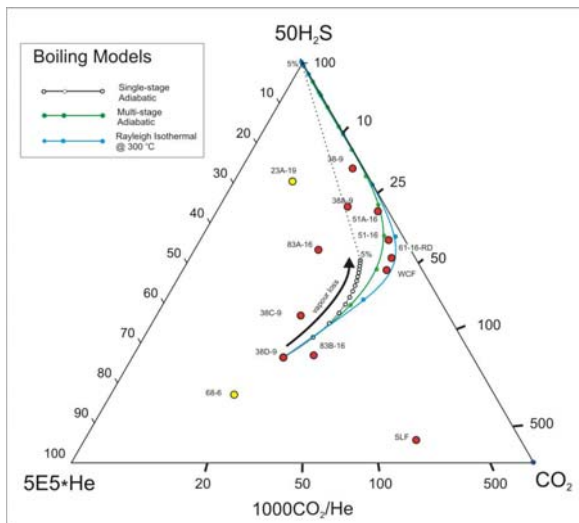


Figure 5. Relative CO₂-H₂S-He compositions compared to theoretical boiling pathways for a 38D-9 fluid composition.

It is of interest to note that both the most- and least-degassed fluids (38-9 and 38D-9 respectively) are from adjacent wells in the East Flank, suggesting that permeability in this part of the field is strongly compartmentalized.

The redox state of magmatic-hydrothermal fluids can provide clues, if only qualitative, into the relative proximity of source (i.e., magmatic) component inflows into hydrothermal systems. Two principle redox buffers operate on magmatic hydrothermal system fluids (eg. Giggenbach, 1987). As fluids are released from convectively degassing magma, H₂ fugacities are buffered by two principle magmatic S gas species, H₂S and SO₂. Once magmatic gases are

enveloped into the overlying hydrothermal system, however, water rock interactions involving a di- and tri-valent Fe buffer impose a strongly reducing effect on the fluid.

Total discharge H₂/H₂O fugacity ratios are plotted against these buffer relations in Fig. 6, along with an additional rock buffer relation proposed by D’Amore and Panichi (1980). Plotted temperatures for the discharges derive from the H₂/Ar relation of

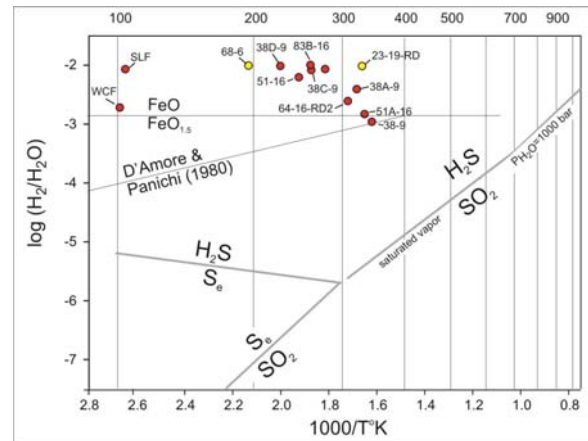


Figure 6. H₂/H₂O fugacity ratio plot for Coso system fluids, compared to main magmatic-hydrothermal redox buffers. Modified from Giggenbach (1987).

Giggenbach (1991). Data for the East Flank wells and fumaroles plot close to or above the so-called FeO-FeO_{1.5} rock buffer, suggesting reducing reservoir conditions are extant in the production reservoir. This is further supported by other calculations showing that CO₂/CH₄ ratios are also

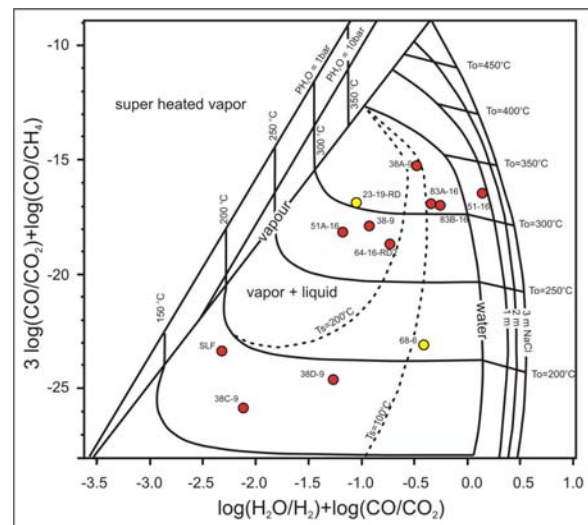


Figure 7. CO₂-CO-CH₄ geoinicator plot. Modified from Chiodini et al., 2001.

governed by these rock buffers. The fact that many of the discharges have marginally higher H_2/H_2O fugacity ratios than dictated by the $FeO-FeO_{1.5}$ rock buffer points to the excess vapor fractions entering the well bores. It can be concluded, at least qualitatively, that based on the reduced nature of the fluids, none of the production zones are immediately proximal to the degassing magma source.

$CO_2-CO-CH_4$ equilibrium relations in the discharges are portrayed in Fig. 7 (adapted from Chiodini et al., 2001). With the exception of the discharge from 51-16, all fluids plot in the two-phase region of the diagram, with the highest East Flank equilibrium temperatures being found in gases from wells 38A-9, 83A&B-16 and 51-16. The 51-16 discharge plots in the single-phase liquid region, which may relate to the dilution effect of injectate water on the log (H_2O/H_2) term in the abscissa. Fluids from 38C-9 and 38D-9 have the lowest equilibrium temperatures, consistent with their having boiled the least of any fluids on the East Flank.

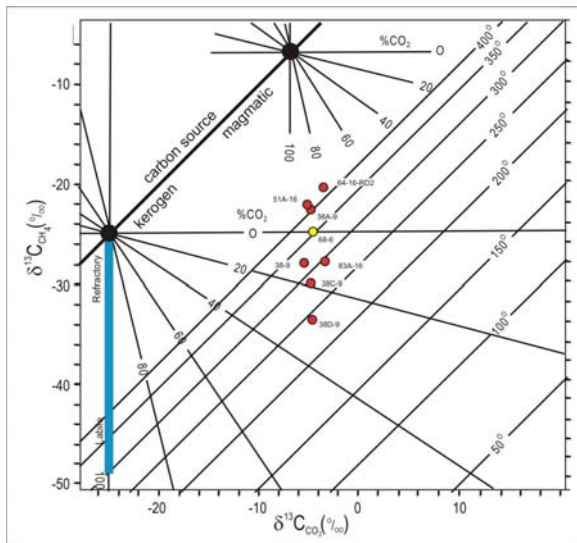


Figure 8. $\delta^{13}CO_2$ and $\delta^{13}CH_4$ signatures for discharges plotted against equilibrium fractionation isotherms and magmatic and kerogen source compositions.

The temperature dependence of ^{13}C fractionation between CH_4 and CO_2 can be used to good effect as a “deeply-focused” geosignature in systems having a single homogenous source of C (eg. Fiebig et al., 2004; Christenson et al., 2002). Discharge data for which reliable $\delta^{13}CH_4$ values were obtained are shown in Fig. 8, where they are plotted against their respective $\delta^{13}CO_2$ signatures, and compared to two potential C source end-member compositions. $\delta^{13}CO_2$ values range from -3.3 to -5.3 across the East Flank, overlapping the generally accepted range for mantle-derived carbon of -4 to -8 (eg. Deines and Gold, 1973). $\delta^{13}CH_4$ values, on the other hand,

ranges from -20 to -34, reflecting either temperature-dependent equilibrium fractionation, or perhaps the existence of multiple sources of C in the reservoir rocks. The highest indicated temperatures range from 420° to 440 °C, are well above either measured or other indicated temperatures. The lower temperatures (eg. 38C-9, 38D-9) match more closely the measured or indicated values.

The present assumption, and one which is consistent with the predominantly igneous and high-temperature metamorphic lithologies thus far encountered in drilling on the East Flank (eg. Kovac et al., 2005), is that there are not multiple sources of C in the reservoirs. The highest indicated temperatures are therefore thought to represent kinetically quenched values from greater reservoir depths, which coincide with the plastic-brittle transition temperature range for dioritic rocks (eg. Fournier, 1999).

Source Characteristics

There is little question that the volatiles derive from a magmatic source in the Coso system. He in the discharges have $^3He/^4He$ ratios which clearly point to a mantle source (Fig. 9a). The lowest $CO_2/^3He$ ratios analyzed in 2005 were ca. 3×10^9 in well 68-6 (Navy I compartment), which is only marginally above the generally accepted MORB value of 2×10^9 (eg. Marty and Zimmerman, 1999). The East Flank values range from ca. 5×10^9 to greater than 100×10^9 , once again pointing to the effects of variable amounts of vapor loss from those fluids. The difference in $CO_2/^3He$ values between the 68-6 discharge and the least boiled fluid from the East Flank (38D-9) equates to less than 1 % vapor loss in an open system (ie. Rayleigh) degassing regime at 300 °C. The largest departure (to 51A-16) equates to ca. a 4 % vapor loss under the Rayleigh model.

Of particular interest is the effect that even such small amounts of vapor loss appear to have on the apparent $^3He/^4He$ ratios in the remaining fluid. The curved pathway prescribed by the data point to an *apparent* boiling-induced fractionation of 3He out of the system, equating to decreased $^3He/^4He$ ratio of approximately 2 R/Ra. We currently view this shift to be the result of matrix-fracture transfer of radiogenic 4He formed in the reservoir rock, a process which has also been proposed to account for the declining $^3He/^4He$ ratios in the Geysers production reservoir with time (Dobson et al., 2006).

Relative concentrations of N_2-Ar and He are shown in Fig. 9b, where they are compared to compositions for air, air saturated water (asw), mantle, and arc-type components (Giggenbach, 1987). Also shown are actual data for some NZ arc-type geothermal and volcanic discharges. The Coso data plot along a trend suggesting 2 component mixing between

air/ASW and a N₂-enriched mantle gas with a N₂/He ratio of ca. 200.

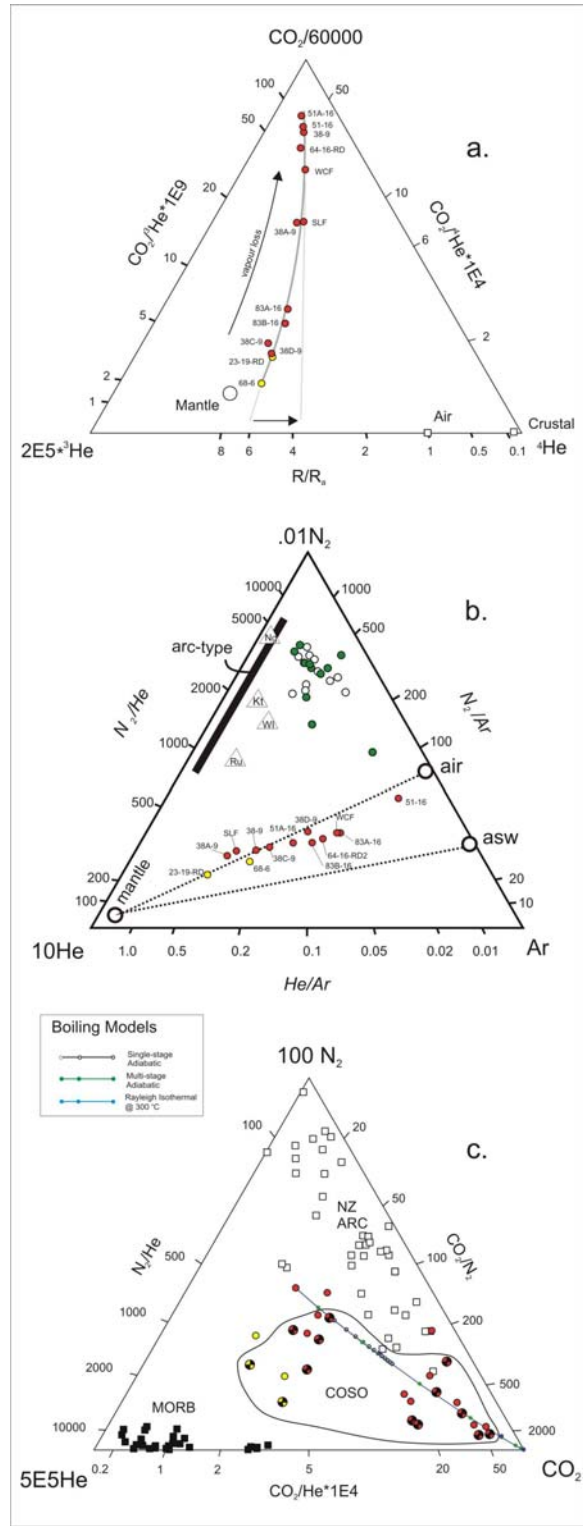


Figure 9. Relative discharge compositions compared to end member source characteristics for: a.) CO₂-³He-⁴He; b.) N₂-He-Ar; and c.) N₂-He-CO₂ systems.

Relative concentrations of CO₂, N₂ and He are shown in Fig. 9c where they are compared to a wider variety of arc discharges from NZ, and to a set of data for MORB basalts (Marty and Zimmerman, 1999), and the 3 boiling pathways described above. It is clear that reservoir boiling cannot account for the apparent enrichment in N₂ in the Coso samples over the MORB values. Even correcting for N₂ introduced with meteoric water (red and black symbols), the Coso gases remain N₂-enriched over their MORB counterparts. This enrichment raises some interesting questions as to the nature of the mantle underlying this nascent core complex at Coso, including whether it carries relict volatile signatures from an earlier subduction zone regime once active along the western margin of North America.

CONCLUSIONS

The results of this study provide some insights into the proximity of heat source inflows in the East Flank, and into the nature of the heat source itself. There is a surprising amount of variability of fluid chemistry over the relatively small production area, and while some of this can be explained as exploitation effects, there is seemingly clear evidence of compartmentalization of production zones.

Interestingly, nearly all of the wells studied (with the exception of 38C-9 and 38D-9) show evidence of having tapped high temperature inflows at some time in the past, based on the different geo-indicators applied in this study. Given that the various equilibria applied here are kinetically controlled, these apparent inconsistencies almost certainly relate to how the system has evolved in the recent geologic past, and how it is now responding to the current exploitation (eg., conversion to a 2-phase vapor-liquid, or in time, even a vapor-static regime).

The highest indicated temperatures from ¹³CO₂-¹³CH₄ fractionation point to values that reach and even exceed those of the plastic-brittle transition for silicic rocks. Gases carrying these highest signatures derive from feed zones supplying 51A-19, 38A-9 and 64-16-RD2. It is suggested herein that the high temperature feeds carrying such signatures into these wells should be considered as the most direct conduits to the heat source.

³He/⁴He isotope ratios reported here show evidence of matrix-fracture transfer of radiogenic ⁴He, which is most likely a direct result of exploitation-induced reservoir boiling. While this has been proposed to explain similar changes in other producing geothermal systems, this also has interesting ramifications for natural systems which undergo depressurization, such as periodically erupting volcanoes.

Finally, apart from N₂, the Coso system discharges which are least affected by boiling have component signatures most similar to MORB gas compositions. N₂, on the other hand, appears to be enriched relative to MORB, possibly reflecting a (relict?) inhomogeneity in the mantle beneath this portion of California. Current work on δ¹⁵N composition on the N₂ may provide some clues as to the origin of this unusual signature.

ACKNOWLEDGEMENTS

This work was supported by the New Zealand Foundation for Research, Science and Technology Contract CO5X0201 and by a New Zealand Royal Society ISAT Linkages Fund travel grant. This work was also supported by the U. S. Department of Energy, Office of Basic Energy Sciences and Office of Geothermal Technologies under contract DE-AC02-05CH11231. We also thank Brandon Johnson for assistance in the field.

REFERENCES

- Adams, M.C. (2004) Use of naturally-occurring tracers to monitor two-phase conditions in the Coso EGS project. *Proceedings 29th Workshop on Geothermal Engineering, Stanford University*, 37-41.
- Arnorsson S. and Sigurdsson, S. (1982) The chemistry of geothermal waters in Iceland. I. Calculation of aqueous speciation from 0° to 370°C. *Geochimica Cosmochimica Acta* 46, 1513-1532.
- Chiodini G., Marini L. and Russo M. (2001) Geochemical evidence for the existence of high-temperature hydrothermal brines at Vesuvio volcano, Italy. *Geochimica Cosmochimica Acta* 65, 2129-2147.
- Christenson, B.W., Mroczek, E.K., Kennedy, B.M., van Soest, M.C., Stewart, M.K. and Lyon, G., (2002) Ohaaki reservoir chemistry: Characteristics of an arc-type hydrothermal system in the Taupo Volcanic Zone, New Zealand. *Journal Volcanology Geothermal Research* 115, 53-82.
- D'Amore F. and Panichi C. (1980) Evaluation of deep temperature of hydrothermal systems by a new gas-geothermometer. *Geochimica Cosmochimica Acta* 44, 549-556.
- Deines P. and Gold D.P. (1973) The isotopic composition of carbonatite and kimberlite carbonates and their bearing on the isotopic composition of deep-seated carbon. *Geochimica Cosmochimica Acta* 37, 1709-1733.
- Dobson P., Sonnenthal E., Kennedy M., van Soest T. and Lewicki J. (2006) Temporal changes in Noble gas compositions within the Aidlin Sector of the Geysers Geothermal System. *Geothermal Resources Council Transactions* 30, 903-907.
- Fiebig, J., Chiodini G., Caliro S., Rizzo A., Spangenberg J. and Hunziker C. (2004) Chemical and isotopic equilibrium between CO₂ and CH₄ in fumarolic gas discharges: Generation of CH₄ in arc magmatic-hydrothermal systems. *Geochimica Cosmochimica Acta* 68, 2321-2334.
- Fisher, T.P. and Marty, B. (2005) Volatile abundances in the sub-arc mantle: insights from volcanic and hydrothermal gas discharges. *Journal Volcanology Geothermal Research* 140, 205-216.
- Fournier, R.O. (1999) Hydrothermal processes related to movement of fluid from plastic into brittle rock in the magmatic-epithermal environment. *Economic Geology* 94, 1193-1212.
- Fournier, R.O. and Thompson, J.M. (1982) An isotopic study of the Coso, California, Geothermal Area. *Geothermal Resources Council Transactions* 6, 85-87
- Giggenbach, W.F. (1987) Redox processes governing the chemistry of fumarolic gas discharges from White Island, New Zealand. *Applied Geochemistry* 2, 143-161.
- Giggenbach, W.F. (1991) Chemical techniques in geothermal exploration. *In Application of Geochemistry in Geothermal Reservoir Development, UNDP/UNITAR Series of Technical Guides on the Use of Geothermal Energy, Rome.*
- Giggenbach, W.F. (1995) Variations in the chemical and isotopic compositions of fluids discharged from the Taupo Volcanic Zone: a review. *Journal Volcanology and Geothermal Research* 68, 89-116.
- Giggenbach, W.F. (1997) Relative importance of thermodynamic and kinetic processes in governing the chemical and isotopic composition of carbon-gases in high-

heat/flow sedimentary basins. *Geochimica Cosmochimica Acta* 61, 3763-3785.

- Hilton, D.R. (1996) The helium and carbon isotope systematics of a continental geothermal system: results from monitoring studies at Long Valley caldera (California, USA). *Chemical Geology* 127, 269-295.
- Kennedy, B.M. and Truesdell, A.H. (1996) The Northwest Geysers high-temperature reservoir: evidence for active magmatic degassing and implications for the origin of the Geysers geothermal field. *Geothermics* 25, 365-387.
- Klein, C.W. (2000) User-oriented software for geothermal applications: The WATCHWORKS program for Windows 95. *Proceedings World Geothermal Congress 2000, Kyushu-Tohoku, Japan, May 28-June 10, 2000*.
- Kovac, K.M., Moore, J.N. and Lutz, S.J. (2005) Geologic framework of the East Flank, Coso Geothermal Field: Implications for EGS development. *Proceedings 30th Workshop on Geothermal Engineering, Stanford University*, 486-492.
- Lees J.M. (2002) Three-dimensional anatomy of a geothermal field, Coso, southeast-central California. *GSA memoir* 195, 259-276.
- Marty, B. and Zimmermann, L. (1999) Volatiles (He, C, N, Ar) in mid-ocean ridge basalts: Assessment of shallow-level fractionation and characterization of source composition. *Geochimica Cosmochimica Acta*, 63, 3619-3633.
- Monastero, F.C., Katzenstein, A.M., Miller, J.S., Unruh, J.R., Adams, M.C. and Richards-Dinger, K. (2005) The Coso geothermal field: A nascent metamorphic core complex. *GSA Bulletin*, 117, 1534-1553.
- Quisefit, J.P., Toutain, J.P., Bergametti, G., Javoy, M., Cheynet, B. and Person, A. (1989) Evolution versus cooling of gaseous volcanic emissions from Momotombo Volcano, Nicaragua: Thermochemical model and observations. *Geochimica Cosmochimica Acta* 53, 2591-2608.
- Williams, A.E. and McKibben, M.A. (1990) Isotopic and chemical constraints on reservoir fluids from the Coso Geothermal Field, California. *Geothermal Resources Council Transactions* 14,1545-1552.